IJCS INTERNATIONAL JOURNAL OF CONSERVATION SCIENCE
ISSN: 2067-533X Volume 11, Issue 4, October-December 2020: 965-978 www.ijcs.ro

PEWTER FILLED SEASHELL COINS FROM CENTRAL INDIA (500 BC – 11TH CE) – SURFACE MORPHOLOGY AND MICRO-STRUCTURE

Meenakshi MALUSARE[1], Manager Rajdeo SINGH[2*]

[1] National Museum Institute, Janpath, New Delhi-110 011, India
[2] National Research Laboratory for Conservation of Cultural Property, Aliganj, Lucknow 226024, India

Abstract

Pewter filled seashells were used as coinage in Central India from 500 BC to 11th CE when seashells or cowry were common numismatic until 17th-18th CE in all the continents. The present paper is based on examining of three pewter-filled cowry coins collected from the central Indian state of Madhya Pradesh. The analytical investigations were performed through the ED-XRF, XRD, and SEM-EDX analysis of the coins. The X-ray elemental mapping for the coin surface, as well as the cross-sectional area, was carried to understand the composition of the pewter. Scanning electron microscope coupled with energy-dispersive X-ray analysis was used to study the surface topography and microstructure/inhomogeneity within the coins matrix, and elemental composition was recorded. ED-XRF revealed a concentration gradient on the coin surface to that of composition in bulk. The mineralization of lead, tin, copper, and iron was observed on the coin surface through XRD analysis. Investigations showed the presence of a high concentration of impurities of Fe, Zn, Cu and Sb in the coin matrix due to imperfect metallurgical process. The formation of the tin island in the matrix of the coin was recorded from the cross-sectional analysis due to the improper mixing of component materials and the separation of different phases during solidification.

Keywords*: Pewter; Cowry coins; Inhomogeneity; Tin island; Cross-section; Metallurgical process; Elemental composition*

Introduction

Seashells were used as a medium of exchange, similar to coins in almost all continents of the world [1]. The shell money initially consisted of either whole seashells or their pieces. Among the variety of shells used as coins, shell type Cypraeamoneta, locally named cowry, had a great international demand and was abundantly available in the Indian Ocean [2, 3]. In ancient times, these shells were mostly collected from the coasts of Maldives, SriLanka, West Coast of India, and other East Indian Island for use as money [2, 4]. Cowry shell money was an important part of trade networks of Africa, South Asia, and East Asia [5]. Inscriptions and archaeological evidence show that the cowry shell was an important object of value in the China Shang Dynasty (C.1766-1154 BC) [6]. In the East Indian state of Odisha, cowry was used as currency till 1805 when it was abolished by the British East India Company [7]. Due to their great strength, durability, easy to handle, and transport – cowry became valued as metal coins. Besides, their specific shapes and the distinctive texture was the best protection against forgery.

* Corresponding author: m_singh_asi@yahoo.com

To enhance the value of the cowry shell and undo its lightweight, in around 500 BC, when the evolution of coins was not there, lead-filled seashells were used as coinage in the central part of India [8]. For the purpose, a hole was created by breaking the top smooth surface of the seashell and liquid compound of lead was filled into for use as currency. The metal filling was done to the top layer to make the surface even and in some instances, the natural hole on the reverse of the shell was also filled to make it water impermeable. This was done because the coins can easily be differentiated from the common seashells and may also be used as money for trade. Though the seashells or cowry were used all over the world as money till late 17^{th} - 18^{th} CE, the lead-filled seashells were mostly used in India's central part and adjoining areas. The coinage belongs to the period ranging from 500 BC to 11 CE. This paper deliberates on three numbers of metal filled cowry coins collected by the author (MS) from the central Indian state of Madhya Pradesh.

To understand the history and culture of the past, there is now growing interested in dedicated archaeological research on numismatist's works. The visual examination is insufficient to classify the coins which require elemental analysis. The investigations on the chemical composition of ancient coins lead to valuable information regarding manufacturing technology, age, authenticity, and corrosion products [9, 10]. The composition of major elements provides useful information about the history, economic condition, and material and technology applied to produce of metal alloys [11].

The trace elements in the coins indicate about the ores sourced and manufacturing procedure adopted [12]. The composition of ancient coins also helps to distinguish between the original and the fake. Almost all the techniques employed for the chemical composition of the coins are non-invasive or need a minor fraction of the coin surface for study [13–15]. However, the chemical composition of the coin surface may have changed over time by the corrosion process. It may reveal great-divergence from the composition of the core [16, 17] The second reason for inhomogeneity in metals is the depletion of the more chemically active phase in contact with the less active phase [18, 19]. Further, certain impurities in the ores may have been difficult to remove. Sometimes alloy addition is made in the metal with the purpose of loweing the melting point or to make the final alloy more or less malleable. The removal of tiny flakes of metal from the surface usually exposes the underlying metal, which is representative of the original composition [14] with some exceptions.

It is rare to find artifacts of pure tin in archaeological sites. Tin is more often found in various alloys, particularly in combination with copper for bronzes or tin pewter [20]. Tin seldom survives in archaeological sites due to its transformation into a mix of stannous and stannic oxide (SnO and SnO_2) by direct intercrystalline oxidation [21]. Tin can also be lost form artifacts as it forms loose powdery grey tin, commonly referred to as a, tin pest by allotropic modification [22]. The presence of sodium chloride stimulates the corrosion of tin [23]. In anaerobic environments in the presence of sulfate-reducing bacteria tin can transform into tin sulfate.

Lead is mostly used for weight and commonly found in shipwrecks, cannonballs, sheeting, coins, etc. Lead is stable in neutral or alkaline condition especially if carbonates are present in the surroundings [24]. On prolonged atmospheric exposure, lead forms basic lead carbonate ($2PbCO_3$, $Pb(OH)_2$, lead oxide (PbO and PbO_2), and lead carbonate. Lead oxide generally forms a protective layer on the artifacts that prevents further oxidation. In the marine environment, along with the above corrosion, product, lead also forms lead chloride ($PbCl_2$), lead sulfide (PbS), and lead sulfate ($PbSO_4$) [25]. A mix of lead and tin called pewter is filled in a cowry shell for weight and increases its value. As lead and tin can be melted easily at low temperature (172-230°C), it was specifically exploited by ancient civilization as filling material for seashell coinage. Pewter is a malleable alloy, and traces of copper, bismuth, and zinc, if present as, impurities act as a hardener for pewter. The high concentration of lead leads to a lower grade of pewter.

The other reason for filling pewter in the seashell is that it gives protection to its handler from the toxic impact of lead as being malleable the metal may cause death if consumed through the food chain. The lead poisoning was a common disease, and the presence of traces of lead have been reported through bone analysis of ancient civilization [26, 27].

It is observed that lead pewter, an alloy of lead and tin, always survives in better conditions than lead-free pewter [28]. This is more likely due to the formation of lead corrosion product that protects the surface of the object. Lead-free pewter often completely mineralized to stannic oxide (SnO_2), and various other mineralized compounds are formed specifically in aerobic conditions. However, both lead and lead-free pewter survive in good condition by forming protective layers [29].

This paper is aimed to study the microstructure of pewter filled seashell coins collected from central India. The chemical composition and corrosion behavior of the alloy has been studied to ascertain reasons for its survival, mixing technology, metallurgical process, and ores used for the extraction of the metals. The other important area to look for the coins is why it was filled in a seashell hole and why pewter alloy coins were fabricated separately. Did the calcium carbonate layer of the seashell helped preserve the coins from further mineralization? We have used analytical instruments like XRF, XRD and SEM-EDX to characterize the materials for the coins and to study its composition and corrosion behavior. The results obtained from these analytical investigations will help find the correlation between the chemical composition of the coins and offer complementary information to archaeologists, art historians, and conservation professionals [30]. By SEM-EDX analysis, the deposition of higher metal content, and its effect can be investigated, and examination under XRD will help in studying the structural, and surface morphology studies of the pewter-filled sea-shell coins [31, 32].

Materials and Methods

The general obverse/reverse view of pewter filled cowry coins is shown in figure 1. As we could collect only three metal-filled seashell coins, this investigation is based on studies undertaken on these coins only. Photographs of the coins clearly show metallic filling on the top surface by manually creating a hole by breaking the seashell on top (Fig. 1). An even level has been maintained on the top surface after metallic fillings. The reverse side of the cowry has also been filled with the same material probably, to make the coin water impermeable. The weight of each coin varies between 4.4 to 8.1g, as shown in Table 1. The dimension of the coins is also shown in Table 1.

Table 1. Dimensions of the pewter filled seashell coins

Name of the coin	Weight (in g)	Size (in cm) (length/width/thickness)
Coin No.1 (SK1)	4.4g	1.3cm/0.8cm/0.4cm
Coin No. 2 (KH3)	4.9g	1.3cm/0.9cm/0.4cm
Coin No. 3 (BK1)	8.1g	1.6cm/1.1cm/0.6cm

The weight of the coin has a linear relation to its dimension as bigger the cowry more pewter was filled in it. The amount of alloy material filled also depends on the dimension of the hole created on the top surface of the cowry. Poor quality control appears to have been exercised the coins varied in weight, dimensions, and chemical composition. For the chemical composition of the coins, the ED-XRF method (Model: BrukerXFlash 6I30) was used, which is rapid, multi-elemental, non-destructive, that does not require sample preparation. As the geometry of the sample plays a decisive role in the quantitative ED-XRF analysis, the flat regions of the coins were analyzed. At least four measurements for each coin were taken and

data averaged for XRF analysis. As the X-ray cannot penetrate the sample, more than few tens of micrometer [19] and the surface analysis may not provide data for the bulk composition, a 0.5mm flake was removed from the coin surface to get the representative composition of the bulk [5].

To characterize the composition and nature of corrosion products, the X-ray diffraction method was utilized. The XRD method is nondestructive, reproducible, and fast, and can be used for both polycrystalline and amorphous coatings having thicknesses up to several micrometers [33]. The XRD analysis of the coins was carried with an advanced fourth-generation powder x-ray diffractometer system, the Rigaku Mini Flex II. With the Rietveld technique, the produced pattern was refined, and measured values were compared with the calculated data stored in an International Centre for Diffraction (ICDD) data bank.

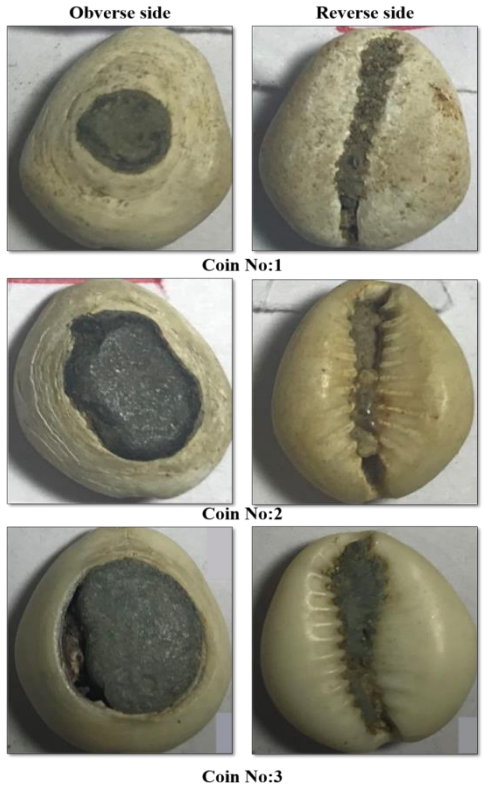

Fig. 1. General view of obverse/reverse surface of pewter filled seashell coins from Central India

Ancient coins generally possess a rough homogenous core and mostly thin surface layer with different compositions and varying thicknesses. The energy dispersive x-ray microanalysis using a scanning electron microscope (SEM-EDX) in the limited case is allowed where sectioning of the coins is permitted. The high magnification provided by a scanning electron microscope is used to investigate the microstructure, homogeneity/heterogeneity of the coins, and chemical composition of the core from the areas of the coins not affected by the corrosion [31]. The practical use of this method, in association with other analytical techniques, provides valuable information about the chemical composition of ancient coins.

A detailed morphological characterization and chemical identification of the coins were obtained by Scanning Electron Microscope. The SEM-EDX analysis was carried out by Carl Zeiss EVO50 scanning electron microscope at various magnifications at high vacuum mode.

Scanning electron microscope coupled with the EDX instrument of Bruckerwas used for analysis. The accelerating voltage was set at 20kV at a working distance of 8mm at a resolution of 2250nm. The EDX data was processed with Roentag software. Additional investigation was carried out by SEM-EDX on the cross-section of the specific fragments of the coins.

Results and Discussion

Chemical composition of the coins

To investigate the composition of the coins and any surface inhomogeneity, the coin was subject to point analysis by ED-XRF on the surface and the inner part after removing a small flake of 0.5mm thick surface layer. The removal of a thin layer of the metal from the surface of the coin exposed metal that is the representative of the composition of the bulk. The XRF data is shown in Table 2.

Table 2. XRF analysis of the seashell coins

Sample No.		Elemental composition weight in percentages (%)						
		Ca	Fe	Cu	Cl	Sn	Pb	Zn
Coin No. 1 (SK1)	Surface layer composition	-	2.78	1.44	1.07	5.65	87.99	1.36
	Bulk composition	-	-	2.60	-	4.07	91.72	-
Coin No. 2 (KH3)	Surface layer composition	-	3.86	7.72	0.91	5.60	78.18	3.70
	Bulk composition	-	5.58	-	-	1.80	86.49	6.14
Coin No. 3 (BK1)	Surface layer composition	0.39	0.89	1.24	-	5.35	91.90	1.96
	Bulk composition	-	0.77	-	-	2.85	94.40	1.96

The data show large variations in the concentration of the element in the coins. The analysis shows the Pb and Sn as the main elements which form the bulk composition and their metallurgy. Other elements like Fe, Cu, Zn, Ca, Ti and chloride were detected as minor/trace elements. The Pb content of the bulk is always larger than the value measured on the surface, mainly due to preferential mineralization of lead at the surface. Since the surface contains about 2.73% to 8.31% less than the percentage of Pb in bulk, this can be attributed to the contamination and oxidation process the coins have been subjected to in the past. The absence of silver in the Pb-Sn alloy in the analyzed coins indicates that lead was either extracted from “non- argentiferous galena" or silver was perfectly extracted during the metallurgical process of the ores. The tin content on the coin surface is always higher than the composition in bulk by a percentage of 1.59 to 3.80 (Table 2). It appears that the content of lead on the surface and its corrosion products in the form of PbO, PbO_2, has worked as a protective coat for the tin to mineralize in bulk. Tin has concentrated much on the surface during the solidification process after the molten alloy was poured in the seashell hole. The other minor/trace elements in the composition originated mainly from the different ores or varying manufacturing processes used for Pb/Sn production [32, 33]. All the coins show an amount of copper either as contaminant or in high content in bulk composition. On the coin surface, the Cu content is lower to its concentration in the bulk, again due to the presence of oxidized species on the surface that occurred due to the tendency of copper to dissolute in the corrosion layer [34]. As copper and lead phase is exposed to the surface, the lead has corroded preferentially. However, as soon as the given lead phase is consumed, the copper prevents further corrosion of lead as the copper phase first corrode before additional lead is exposed to the surface. Copper is present in all the coins, and the percentage varies from 1.24% to 7.72%. Zinc is present in a high percentage in coin no. 2 and 3, and content varies from 1.36% to 6.14 %. Lead is usually found in ore

associated with the metals like Zinc, Silver and Copper and it is extracted together with these metals. Lead is extracted from its ore by reduction with carbon. It appears that impurities like Zn and Cu could not be separated during the metallurgical process of lead ore and quite impure lead was used for mixing in pewter. The presence of iron in all the coins, and iron content varies from 0.77% to 5.58% in the coins. Iron is mostly present as an impurity in tin ore and is removed by the electromagnetic process. During the extraction of Sn from its ore by the carbon reduction process, the iron impurities could not be separated from the pure metal. This indicates that the raw materials for the pewter remained mostly contaminated with impurities due to a lack of proper extraction process. The surface of coin no 1 and 2 shows the presence of chlorides (0.97-1.07%) during exposure of the coins in its environments. The presence of chloride on the coin surface has stimulated corrosion of tin at its top surface, also observed through the XRD analysis of the coins.

XRD Analysis of the Coins

The XRD pattern of three coins is shown in figure 2. The Crystalline phases observed in coin no.1 as corrosion products are mainly PbO, PbO_2, SnO, CuCl, $CuCl_2$, and Fe_2O_3 (Fig. 2a).

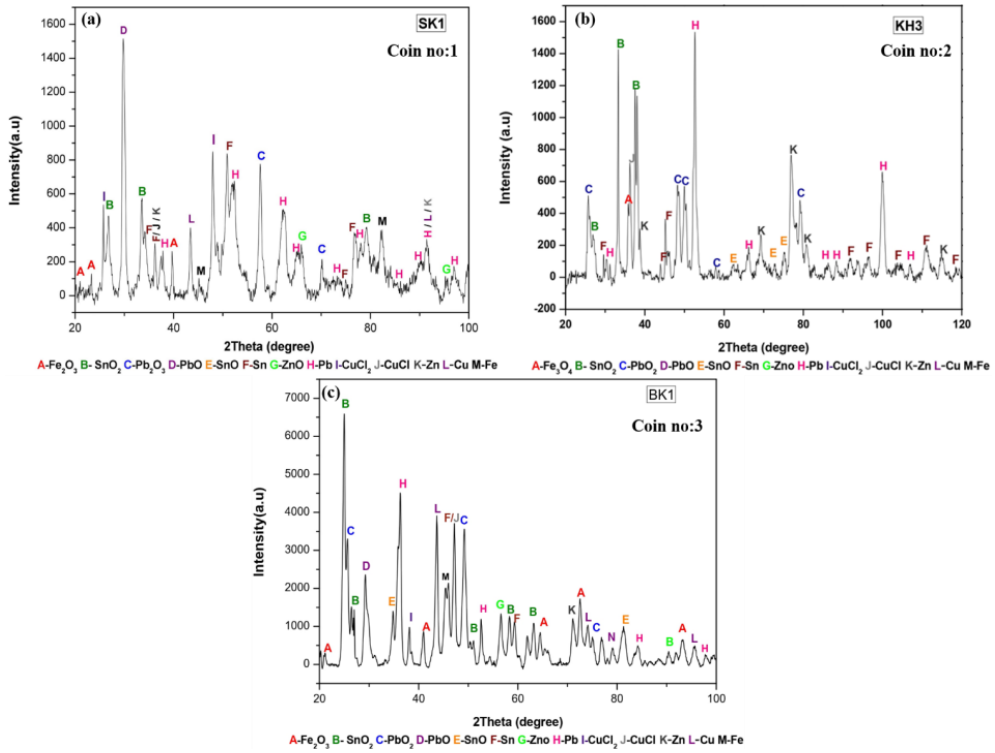

Fig. 2. XRD diffractograph of the pewter filled seashell coins 1 – 3

The lead corrosion product on the surface of the coins has given protective coatings to intense mineralization of tin in bulk on the surface. Copper mineralization products in the form of CuCl and $CuCl_2$ are also observed on the coin surface. Iron has also mineralized on the coin surface and formed Fe_2O_3. In coin no. 2, the corrosion product observed on the surface is similar to coin no. 1. However, chloride in the coin surface has caused mineralization of Cu to form CuCland $CuCl_2$. The mineralization of iron in a higher oxidation state of Fe_3O_4 is observed in this coin (Fig. 2b). Tin has mineralized to both stannous (SnO) and stannic oxide (SnO_2) in this coin. In coin no. 3, besides the lead and tin corrosion products, copper mineralization in the form of CuCland $CuCl_2$ was detected through XRD (Fig. 2c). The lead has mineralized to both

PbO and Pb_2O_3. The iron corrosion product in the form of Fe_2O_3 was detected in the coin. Tin has mineralized to both stannous and stannic oxides. Besides, zinc mineralization in the form of ZnO was also identified in this coin. The part of the pewter under the shelter of the seashell layer could not be sampled due to the fear of destruction, and damage to the coins. Hence, the corrosion product formed on pewter inside the shell layer could not be analyzed to compare its behavior vis-à-vis the exposed surface layer. The bulk of the composition remained Pb, Sn, Fe and Zn for the coins.

SEM-EDX Analysis

Leaded pewter often has a concentration gradient because of the separation of the lead-rich phase or tin-rich phase during solidification. Therefore, an additional investigation was carried by Scanning Electron Microscope on the cross-section of the specific fragments of the coins. The performed SEM was compared with the data obtained from XRF analysis. The high magnification SEM photomicrographs of the coin are shown in figure 3a-b. From the micrograph, it is observed that Sn-Pb alloys are different in microstructure from those of single metals. In the case of single metal, most of the crystals observed are of tetragonal shape. However, in Sn-Pb alloys, the rounded shape crystals are observed. This result coincides with previous studies. It has been reported that in the presence of Pb the Sn changes drastically as Pb inhibits the deposition of Sn on Sn and prevents the formation of inherent Sn crystal [35, 36]. Therefore, the rounded shape observed in the microstructure indicates that the Sn-Pb alloys were fabricated by co-deposition of Sn and Pb. Besides, the particles show a variety of size and alloy exhibit more agglomerated forms of particles compared to a single metal.

Many surface cracks on the external surface of the coin are observed in the 4µm image figure 3a along with mineralized particles of lead on the surface. In the image figure 3b hollow structures with an uneven surface and metallic grains of Sn and Pb are visible. The surface of the coins is mostly rough and granular structure is visible at higher magnification.

SEM photomicrographs (Fig. 3c-d) show the cross-sectional images of coin no. 3 observed to visualize the internal microstructure of the coin. The internal of the coin is marked by forming of islands of tin globule within the matrix (Fig. 3d) with a highly fractured microstructure. The orientation of various grains within the coins can be seen in Figure 3c. From the microstructure, it is observed that pewter has a concentration gradient because of the separation of lead rich and tin rich phases during solidification.

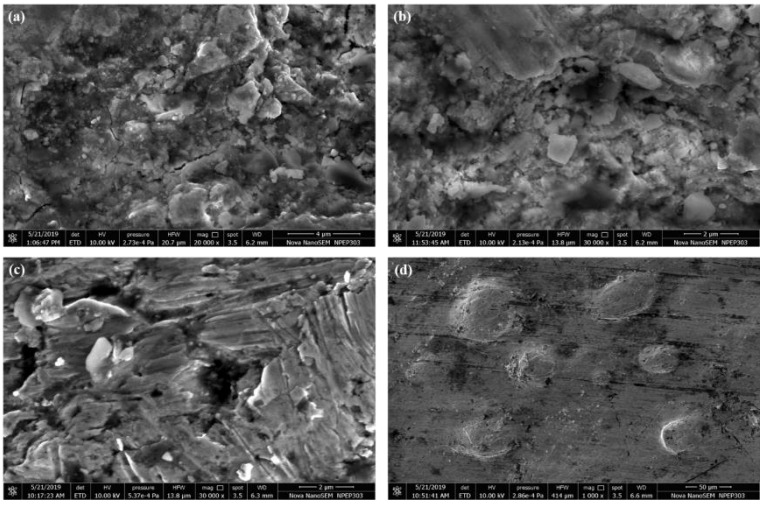

Fig. 3. SEM photomicrograph of pewter coins. Images 3a and b show coin surface, images 3c and d cross sectional view of the coin

Coin No.1

The SEM-EDX spectrum of a coin no. 1 for 8µm and 4µm area is shown in the figure 4a and b. White lead particles, as well as dark color tin particles, were targeted for the EDX data at point no. 8597 and 8598, respectively and the value obtained for coin no 1 is shown in figure 4a and b. The white color particles are mostly made up of oxides of lead (31.54%) and tin (31.58%) with Carbon (5.88%), S (7.14%) and Sb (9.13%) as minor constituents. The other elements present in trace quantities are Si (1.41%), Cl (0.77%), Fe (0.65%) and Zn (0.04%). In the tin-rich phase (Fig. 4b) the major elements detected are tin (63.94%), O (25.46%), Si (5.11%) and Nitrogen (4.05%). The other elements present in trace level are Fe (0.85%), Pb(0.39%) and Cl (0.21%) in the coin.

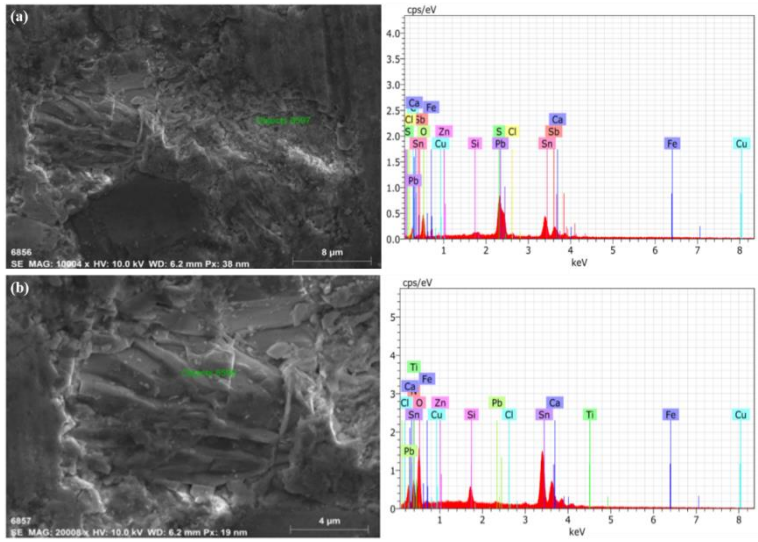

Fig. 4. EDX data of point no. 8597 & 8598 pewter filled Coin no. 1

The points analysed for EDX analysis for coin no.1 were subject to X-ray mapping for the distribution of the elements. The X-ray mapping of the element lead, tin, and other minors/ trace elements are shown in figure 5 for the area analyzed for elemental EDX data (Fig. 4a).

From the distribution of lead and tin in the sample (Fig. 5a) it is observed that there is a formation of lead and tin islands in the sample due to imperfect mixing of the ingredients. The presence and distribution of other components like C, O, Zn and Fe present in the sample as impurities are shown in figure 5b in various shades.

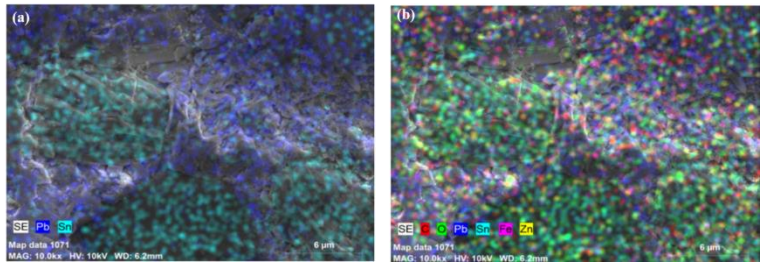

Fig. 5. Elemental mapping of Coin no. 1 (a) distribution of lead and tin (b) multi-element distribution in the coin

From the photomicrograph, it is observed that there is an imperfect mixing of constituent's elements both major and minor in the coin. It can also be observed that ancient workers could not remove impurities like Fe and Zn from the ores of Pb and Sn during the metallurgical process. From the individual elemental mapping on the surface, it is observed that most coins were fabricated by mixing more of tin followed by Pb. Other elements like C, Zn, and Fe are present in low quantity and their distribution in coin no. 1 is shown in figure 6.

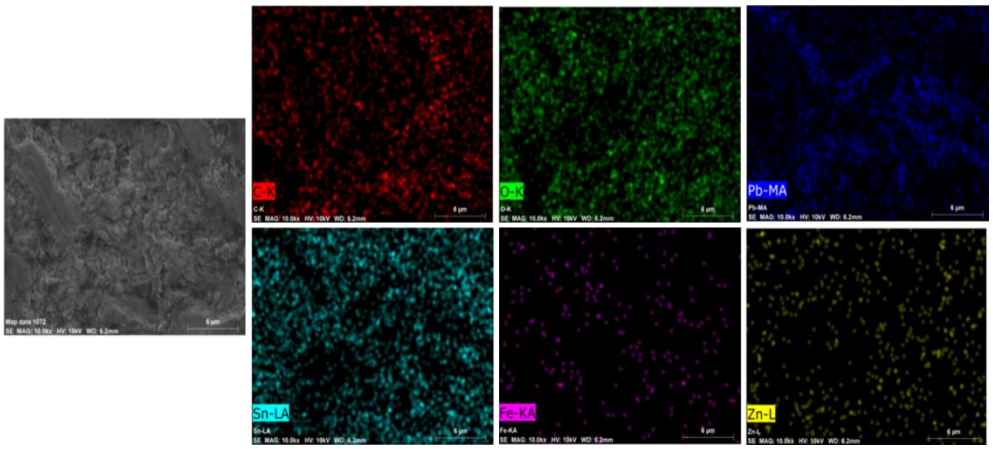

Fig. 6. EDX elemental mapping of C, O, Pb, Sn, Fe and Zn in Coin no. 1

Coin No. 2

The 8µm area of the coin no. 2 was viewed and EDX data recorded at point no. 8603 figure 7a. At this point the coin is mainly composed of Si (23.84%), O (24.74%), C (16.79%), Al (16.31%), Sb (6.16%), Pb (4.03%), Sn (3.64%) and Ca (1.98%). Other elements like Zn, Mg, Cl and Cu were identified as minor constituents of the coins. From the EDX data, it is observed that there is also the presence of aluminum silicates minerals at isolated locations within the coin matrix due to the imperfect metallurgical process. The content of Pb and Sn at such point is considerably low.

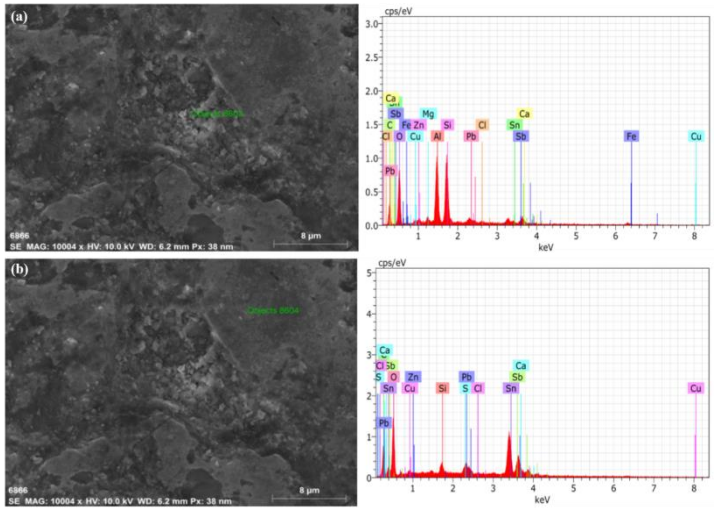

Fig. 7. EDX data of point no. 8603 & 8604 pewter filled Coin no. 2

At another 8µm image of coin no. 2, the point 8604 was viewed and EDX data is listed in figure 7b. The coin at this point is mainly composed of Sn (48.29%), O (18.61%), Sb (4.40%), C (27.49%), Pb (4.99%), Si (2.63%), S (1.75%) and Cu (1.28%). The very high content of carbon in the coin is due to unburntcharcoal, which was probably used in the metallurgical process of reduction of ores. Therefore, the cross-section of the coin shows very indifferent composition at different locations within the matrix.

Another 5µm image of the coin no. 2 was observed under the scanning electron microscope and elemental mapping carried out (Fig. 8a). From the elemental mapping, the uneven distribution of Pb and Sn can be viewed in the coin (Fig. 8b) due to the concentration gradient. The distribution of other impurities like C, O, Fe and Zn within the coin (Fig. 8c) was also recorded.

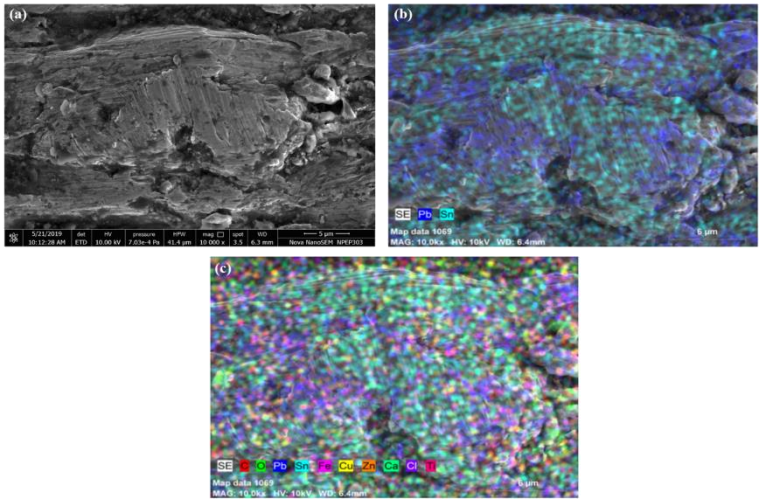

Fig. 8. Elemental mapping of (a) SEM image of Coin no.2
(b) Distribution of lead and tin (c) multi-element distribution in the coin

In table 3 are presented the EDX composition on all the coins.

Table 3. EDX data (wt%) of pewter filled seashell coin no. 1 to 3.

	Coin No.1 (wt%)		Coin No. 2 (wt%)		Coin No. 3 (wt%)	
Element	**Point 8597**	**Point 8598**	**Point 8603**	**Point 8604**	**Point 8594**	**Point 8595**
Sn	31.58	63.94	3.64	48.29	28.16	46.32
Pb	31.54	0.39	4.03	4.99	15.29	16.24
O	11.85	25.46	24.75	18.61	29.16	6.68
Sb	9.13	--	6.16	13.87	--	14.10
S	7.14	--	--	1.75	3.86	3.92
C	5.88	--	16.79	8.55	8.69	6.62
Si	1.41	5.11	23.84	2.63	8.49	3.44
Cl	0.77	0.21	0.41	0.02	0.67	--
Fe	0.65	0.85	--	--	0.87	0.75
Zn	0.04	--	0.95	0.02	0.34	0.48
Cu	--	--	0.20	1.28	--	0.32
Ca	--	--	1.98	--	--	--
N	--	4.05	--	--	--	--
Al	--	--	16.31	--	--	0.84
Mg	--	--	0.93	--	--	0.29
K	--	--	--	--	4.45	--

Coin No. 3

The coin no.3 elemental composition at point no. 8594 in the 3µm image is shown in figure 9a along with its EDX data. It is observed that the white crystalline material mainly consists of Sn (28.16%), Pb (15.24%), O (29.16%), C (8.69%), K (4.49%) and S (3.86%). Other elements like Zn, Fe and Cl are present in minor quantities. The alloy is mainly fabricated by the combination of lead and tin mixture, however, the tin is present in higher quantity than lead at this point. Another 3µm area of the coin no. 3 was viewed under SEM and EDX data for point no. 8595 is shown, figure 9b.

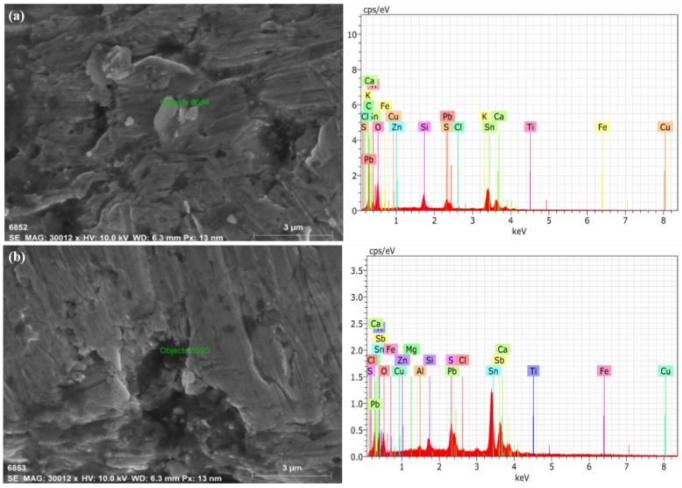

Fig. 9. EDX data of point no. 8594 & 8595 pewter filled coin no. 3

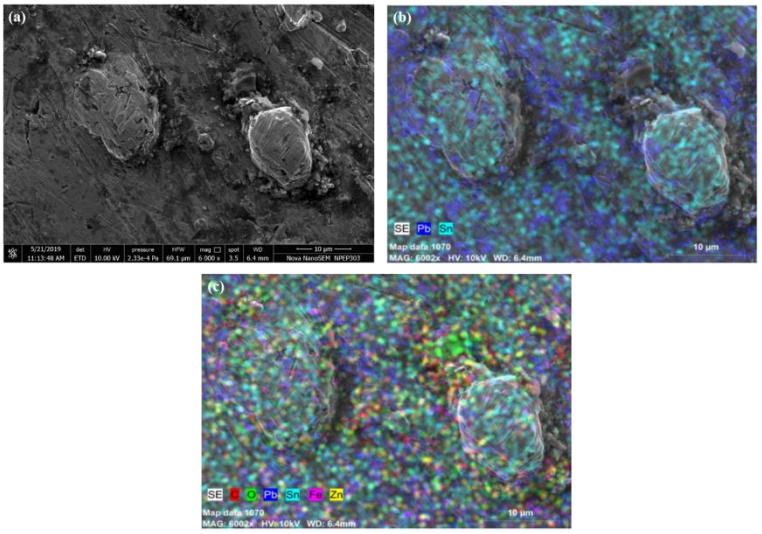

Fig. 10. Elemental mapping of (a) SEM image of coin no. 3
(b) Distribution of lead and tin (c) multi-element distribution in the **coin.**

The black area has the major composition of Sn (46.32%), Pb (16.24%), Sb (14.10%), C (6.82%), O (6.68%), S (3.92%) Si (3.44%). Other elements like Al, Fe, Zn, Mg and Cu are present in minor quantities. From the EDX data, it is observed that the black part of the coin

mainly consists of tin-rich phases followed by Pb, Sb, C, O, S and Si. Impurities like Si, S and Sb are due to the imperfect metallurgical process used for refining the metal. The Sn/Pb ratio for point no. 8594 is 1.84 and for point no. 8595 is 2.85 pointing concentration variations at a different point in the coin due to improper mixing of the alloy elements. By observing a 10µm image of the same coin (Fig. 10) for elemental mapping under X-rays, the distribution of all the major and minor elements are seen. It is observed that the coin is mainly composed of Sn, Pb, C, O, Fe, Cu, Zn, Ca, Cl and Ti with uneven distribution of the elements within the coin. It is observed that lead/tin alloy was not evenly melted as the coin composition shows improper heating.

A 10µm cross-sectional image of the coin no. 3 was viewed under a scanning electron microscope and many globular structures were observed within the coin matrix (Figure 10a). The globular structure was particularly viewed under a 10µm image under SEM and X-ray elemental mapping was carried out. The distribution of Pb and in the globular area is shown in figure 10b and the distribution of all major and minor elements in figure 10c. It is observed that there is the formation of globular islands of tin in this coin matrix due to imperfect mixing. The image is also showing a high percentage of Zn, Fe within the matrix as impurities from the ore/imperfect metallurgical process.

Conclusions

From the investigative result, it is concluded that pewter instead of pure lead was used as filling material for seashells coinage due to its low melting point of less than 230°C. Lead corrosion product has protected large-scale mineralization of tin on the surface of the coins. The coins were found contaminated with chloride, but it did not cause large scale corrosion of the tin. The concentration gradient in respect of Pb and Cu on the coin surface was evidenced to that of composition in bulk. As Pb content in the composition of the coin is considerably high, low-grade pewter was used as filling material for the coins. The high concentration of impurities like Cu, Fe, Zn etc. in the coin indicates the improper metallurgical process. There is the formation of the tin island in the coin matrix observed at a high magnification SEM image due to the improper mixing of the component materials. As the pewter filled seashells are rare to find, this investigation is based on the analytical results of three coins only that deliberate on the metallurgical process used in alloy fabrication.

Acknowledgments

The authors are thankful for the help extended by the scientists of the Department of Metallurgical, and Material Science, IIT, Roorkee and Central Instrumentation Center, Savitribai Phule University of Pune. Special thanks to Mr. Harish Nikul and Prof. Anjan sir for help during the research. We are thankful to Ghanshyam Lal for the help in the analysis of the coins.

References

[1] J.M. Poutiers, *Gastropods*, **FAO species Identification Guide for Fishery Purposes The living Marine Resources of the Western Centeral Pacific, vol. 1**, 1998, pp. 363–648.

[2] S. Tiley, S. Burger, *Cowries in the archaeological and maritime record*, **Strandloper**, 2002, pp. 3–5.

[3] J. Heimann, *Small change and ballast: cowry trade and usage as an example of Indian Ocean economic history*, **South Asia: Journal of South Asian Studies, 3**(1), 1980, pp. 48–69, doi: https://doi.org/10.1080/00856408008722999.

[4] J. Hogendorn, M. Johnson, **The Sell Money of the Slave Trade,** Cambridge University

Press, 1986.
[5] R.S. Wicks, **Money, Markets, and Trade in Early Southeast Asia: the Development of Indigenous Monetary Systems to AD 1400 (Studies on Southeast Asia)**, SEAP Publications, 1996.
[6] B. Yang, *The Rise and Fall of Cowrie Shells: The Asian Story*, **Journal of World History, 22**(1), 2011, pp. 1–25, doi: https://www.jstor.org/stable/23011676.
[7] S.J. Mahmud, **Pillars of Modern India (1757-1947)**, APH Publishing, 1994.
[8] M.K. Dhavalikar, *The beginning of coinage in India*, **World Archaeology, 6**(3), pp. 330–338, 1975, doi: https://doi.org/10.1080/00438243.1975.9979613.
[9] A. Charalambous, *Analytical methods for the determination of the chemical composition of ancient coins*, **Kyprios Character History, Archaeology and Numismatics of Ancient Cyprus**, 2015.
[10] I. Sandu, N. Ursulescu, I.G. Sandu, O. Bounegru, I.C.A. Sandu, A. Alexandru, *Pedological stratification effect of corrosion and contamination products on Byzantine bronze artefacts,* **Corrosion Engineering Science and Technology, 43(**3), 2008, pp. 256-266. DOI: 10.1179/174327807X234688.
[11] I.G. Sandu, S. Stoleriu, I. Sandu, M. Brebu, A.V. Sandu, *Authentication of ancient bronze coins by the study of the archeological patina - I. Composition and structure*, **Revista de Chimie, 56**(10), 2005, pp. 981-994.
[12] M.F. Guerra, C.O. Sarthre, A. Gondonneau, J.N. Barrandon, *Precious metals and provenance enquiries using LA-ICP-MS*, **Journal of Archaeological Science, 26**(8), 1999, pp. 1101–1110, doi: https://doi.org/10.1006/jasc.1999.0405.
[13] I. Liritzis, N. Zacharias, *Portable XRF of archaeological artifacts: current research, potentials and limitations*, **X-ray Fluorescence Spectrometry (XRF) in Geoarchaeology,** Springer, 2011, pp. 109–142.
[14] G. Spoto, A. Torrisi, A. Contino, *Probing archaeological and artistic solid materials by spatially resolved analytical techniques*, **Chemical Society Reviews**, **29**(6), 2000, pp. 429–439, doi: 10.1039/A903358K.
[15] A. Kirfel, W. Kovkrlmann, P. Yule, *Non-Destructive chemical analysis of old south Arabian coins, fourth century BCE to third century CE*, **Archaeometry, 53**(5), 2011, pp. 930–949, doi: 10.1111/j.1475-4754.2011.00588.x.
[16] L. Beck, S. Bosonnet, S. Réveillon, D. Eliot, F. Pilon, *Silver surface enrichment of silver–copper alloys: a limitation for the analysis of ancient silver coins by surface techniques*, **Nuclear Instruments and Methods in Physics Research Section B: Beam Interactions with Materials and Atoms, 226**(1–2), 2004, pp. 153–162, doi:https://doi.org/10.1016/j.nimb.2004.06.044.
[17] J. Condamin, M. Picon, *Influence of corrosion and diffusion on the percentage of silver in Roman denarii*, **Archaeometry, 7**(1), 1964, pp. 98–105, doi: 10.1111/j.1475-4754.1964.tb00603.x.
[18] M. Singh, M.R. Singh, A. Sharma, B. Dighe, *Medieval silver coins of India: Composition and authentication*, **Nuclear Instruments and Methods in Physics Research Section B : Beam Interactions with Materials and Atoms, 436**, 2018, pp. 163–172, doi:https://doi.org/10.1016/j.nimb.2018.09.022.
[19] M. Salmeron R. Schlögl, *Ambient pressure photoelectron spectroscopy: A new tool for surface science and nanotechnology*, **Surface Science Reports, 63**(4), 2008, pp. 169–199, doi: http://dx.doi.org/10.1016/j.surfrep.2008.01.001.
[20] G.Nordberg, B.Fowler, M.Nordberg, **Handbook on the Toxicology of Metals 4th Edition**, San Diego: Academic Press, 2014, pp. 1241–1285.
[21] R.J. Gettens, *Tin-oxide patina of ancient high-tin bronze*, **Bulletin of the Fogg Art Museum**, **11**(1), 1949, pp. 16–26, doi: http://www.jstor.org/stable/4301170.
[22] N. Eastaugh, V. Walsh, T. Chaplin, R. Siddall, **Pigment Compendium: A Dictionary of**

Historical Pigments, Elsevier Butterworth-Heinmann, USA, 2008.
[23] D. Xia, S. Song, J. Wang, H. BI, Y. Jiang, Z. Han, *Corrosion behavior of tinplate in NaCl solution*, **Transactions of Nonferrous Metals Society of Chine**, **22**(3), 2012, pp. 717–724.
[24] X. Cao, L.Q. Ma, M. Chen, D.W. Hardison, W.G. Harris, *Weathering of lead bullets and their environmental effects at outdoor shooting ranges,* **Journal of Environmental Quality, 32**(2), 2003, pp. 526–534, doi: doi:10.2134/jeq2003.5260.
[25] P. Dillmann, D. Watkinson, E. Angelini, A. Adriaens, **Corrosion and Conservation of Cultural Heritage Metallic Artefacts,** 1st Edition, Oxford, UK: Woodhead publishing Limited, 2013.
[26] M.A. Amaya, K.W. Jolly, N.E. Pingitore Jr, *Blood lead in the 21st Century: The sub-microgram challenge*, **Journal of Blood Medicine, 1**, 2010, pp. 71-78, doi:10.2147/JBM.S7765.
[27] M. Jaishankar, T. Tseten, N. Anbalagan, B.B. Mathew, K.N. Beeregowda, *Toxicity, mechanism and health effects of some heavy metals,* **Interdisciplinary Toxicology, 7(**2), 2014, pp. 60–72, doi: 10.2478/intox-2014-0009.
[28] E. Angelini, S. Grassini, S. Tusa, *Underwater corrosion of metallic heritage artefacts*, **Corrosion and Conservation of Cultural Heritage Metallic Artefacts**, 2013, pp. 236–259.
[29] S.E. Dunkle, *Romarchite and other corrosion phases on metal artefacts from the Queen Anne's revenge (1718),* **Virginia Tech**, 2002.
[30] P. Ewa, J. Lekki, J.M. del Hoyo-Meléndez, C. Paluszkiewicz, M. Nowakowski, M. Matosz, W.M. Kwiatek, *Surface characterization of medieval silver coins minted by the early Piasts: FT-IR mapping and SEM/EDX studies*, **Surface and Interface Anaysis, 50**(1), 2017, pp. 78–86, doi: 10.1002/sia.6338.
[31] S. Chandra, G. George, K. Ravichandran, K. Thirumurugan, *Influence of simultaneous cationic (Mn) and anionic (F) doping on the magnetic and certain other properties of SnO2 thin films,* **Surfaces and Interfaces**, **7**, 2017, pp. 39–46, doi:https://doi.org/10.1016/j.surfin.2017.02.008.
[32] A.M. Awad, M.F. Shaffei, O.S. Shehata, H.S. Mandour, H.S. Hussein, *Study the corrosion behavior of both first and second anodized aluminum surfaces electrolytically colored by nickel and tin*, **Surfaces and Interfaces**, **1**, 2016, pp. 1–6, doi:https://doi.org/10.1016/j.surfin.2016.07.002.
[33] F.R. Aliaj, N. Syla, H. Oettel, T. Dilo, *Thickness determination of TiN and TiAl coatings on steel substrates using X-ray diffraction method and their composition measurements by GD-OES,* **Surface and Interface Analysis**, **49**(11), 2017, pp. 1135–1141, doi:https://doi.org/10.1002/sia.6292.
[34] D. Mamania, M.R. Singh, U.S. Lal, *Examination and analysis of Indian silver punch-marked coins employing WD-XRF and other noninvasive techniques*, **Surface and Interface Analysis, 50**(10), 2018, pp. 947–953, doi: https://doi.org/10.1002/sia.6511.
[35] P.J. Smith, **Chemistry of Tin**, 2nd Edition, Springer, London, 2012.
[36] Z. Goffer, **Archaeological Chemistry**, 2nd Edition, Wiley Interscience, New Jersey, 2007.

Received: September 28, 2019
Accepted: September 18, 2020